

# Advanced Electric Vehicle Components for Long-Distance Daily Trips

**Eric Armengaud**<sup>1)</sup>, **Niklas Wikström**<sup>1)</sup>, **Joze Buh**<sup>2)</sup>, **Miguel Dhaens**<sup>3)</sup>, **Sebastian Gramstat**<sup>4)</sup>,  
**Ricardo Groppo**<sup>5)</sup>, **Marius Heydrich**<sup>6)</sup>, **Valentin Ivanov**<sup>6)</sup>, **Matteo Mazzoni**<sup>7)</sup>, **Aldo Sorniotti**<sup>8)</sup>

*1) AVL List GmbH, Graz, Austria; 2) Elaphe Propulsion Technologies Ltd., Ljubljana, Slovenia; 3) DRiV, Sint-Truiden, Belgium;  
4) AUDI AG, Ingolstadt, Germany; 5) Ideas & Motion Srl., Cherasco, Italy; 6) Technische Universität Ilmenau, Ilmenau, Germany;  
7) Brembo S.p.A., Bergamo, Italy, 8) University of Surrey, Guildford, UK*

**ABSTRACT:** This paper introduces a holistic engineering approach for the design of an electric sport utility vehicle focused on the reliable capability of long-distance daily trips. This approach is targeting integration of advanced powertrain and chassis components to achieve energy-efficient driving dynamics through manifold contribution of their improved functions. The powertrain layout of the electric vehicle under discussion is designed for an e-traction axle system including in-wheel motors and the dual inverter. The main elements of the chassis layout are the electro-magnetic suspension and the hybrid brake-by-wire system with electro-hydraulic actuators on the front axle and the electro-mechanical actuators on the rear axle. All the listed powertrain and chassis components are united under an integrated vehicle dynamics and energy management control strategy that is also outlined in the paper. The study is illustrated with the experimental results confirming the achieved high performance on the electric vehicle systems level.

**KEY WORDS:** electric vehicle, in-wheel motor, dual inverter, power electronics, brake-by-wire, electro-hydraulic suspension, vehicle performance

## 1. INTRODUCTION

When as early as one decade ago the electric cars were mainly considered as the solution for urban mobility then nowadays the transportation electrification is encompassing more and more vehicle categories. It concerns also Sport Utility Vehicles (SUV), which demonstrate continuous growth in popularity over the last years<sup>(1)</sup>. However, such typical requirements to SUV operation as high power, increased loading capacity, cross-country capability, and usability for efficient driving in mixed conditions (on urban, sub-urban and highway roads) put serious challenges to corresponding electric vehicle design. One of the possible solutions in this regard is a holistic designing approach focused on implementation of advanced powertrain and chassis technologies to ensure simultaneous effect in both better energy efficiency and improved driving safety and comfort. Such an approach is being realized in the project EVC1000<sup>(2)</sup> by developing systems and components for integrated wheel-centric propulsion architecture and corresponding electric vehicle (EV) management. Next sections of the paper will introduce these components and demonstrate their performance contributing to the targets of safe and comfortable long-distance daily trips.

## 2. OVERALL CONCEPT

Most of known research and engineering efforts, which are targeting the increase of EV mileage, are concentrated around

improved battery technologies and smart charging. However, other vehicle components can also sufficiently contribute to this field. In this regard the presented study considers the battery electric SUV, Fig. 1, as a target car, where the increase of mileage is being achieved through the implementation of the following components:

- Scalable in-wheel motors with compact centralized axle drive based on a SiC technology,
- Active chassis systems including hybrid electro-mechanical / electro-hydraulic brake-by-wire system and electro-hydraulic suspension actuators,
- Integrated control on chassis and powertrain systems with advanced energy management.



Fig. 1 Target electric SUV.

The target EV has the full mass of about 3000 kg and is being equipped with two rear in-wheel motors (IWM). With this powertrain configuration, the SUV should demonstrate maximum speed of 150 km/h and hill-start climbing ability of 30%. For this specification, the development of mentioned components has an operational target to ensure in the aggregate that the vehicle is able to drive long-distance daily trips of up to 1000 km with no more than 90 minutes additional travel time due to charging, and without additional degradation of the components. Next sections of the paper will explain the design of the main components.

### 3. POWERTRAIN COMPONENTS

The powertrain of the target vehicle is based on liquid-cooled outer rotor synchronous in-wheel motors (IWM)<sup>(3)</sup>, Fig. 2. It provides a nominal torque of 650 Nm at 65 kW of power. In boost mode, the maximum achievable torque is 1.500 Nm at 110 kW.

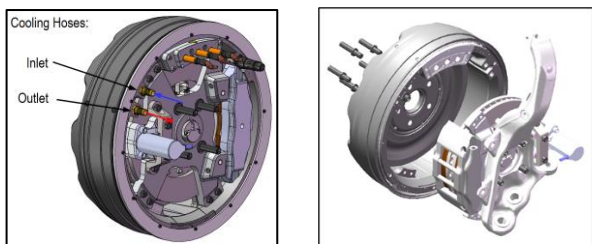


Fig. 2 IWM design.

The proposed IWM design ensures efficient operation with the SiC inverter having switching frequency 50kHz. The paper will outline design optimization process, which resulted in significant system efficiency increase in WLTP cycle evaluation. In particular, maximum motor efficiencies are reached up to 95% with motor WLTP cycle energy drainage (including available regeneration) below 4 kWh, based on estimated mechanical energy of 4.9 kWh needed for the target vehicle during the WLTP cycle.



Fig. 3 Dual inverter.

For the powertrain architecture of the target vehicle, a dual inverter has been developed, Fig. 3, which is able to drive two permanent-magnetized synchronous motors (PMSM), brushless DC (BLDC) or induction motors. It provides continuous input power in excess of 75 kW per motor (150 kW per motor for 10s in Boost-Mode) and can also support the key vehicle management functions as start/stop functionality, multiple interfaces with different accelerator pedal sensors, brake pedal sensors, gear position sensors, and steering angle sensor.

### 4. CHASSIS COMPONENTS

An important contribution to the increase of the EV mileage can be provided by the regenerative braking. In this regard, one of the tasks by designing friction brake system for an EV is to realize a balanced braking architecture ensuring efficient brake blending with the electric motors in a regenerative mode without degradation of the driving safety. To address this point as well as to realize advanced control functions for ABS and ESC systems, a hybrid architecture of the friction brake system is proposed as shown on Fig. 4. The term “hybrid” is used to underline that the system uses two different types of actuation on the calipers: electro-hydraulic actuators on the front axle, and electro-mechanical actuators on the rear driving axle. Moreover, this architecture guarantees a hydraulic fallback level in case of spontaneous power loss, which is a quite important fact in regard of functional safety requirements as proposed in ISO 26262. The response time of both components is below 150 ms. The realized brake torques for the deceleration of 1g are 4046.5 Nm for the front and 1649.7 Nm for the rear wheels, respectively.

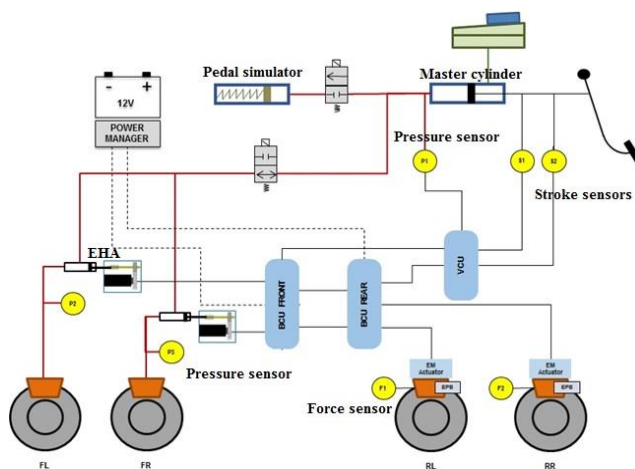


Fig. 4 Architecture of hybrid brake-by-wire system.

The IWMs can negatively affect the ride comfort of an EV in the case of specific road conditions and some driving modes due to increase of the unsprung mass of the vehicle.



Fig. 5 Active suspension layout.

Therefore, an active suspension should be considered by designing of electric SUV chassis. However, the active suspension increases the overall power consumption of the vehicle that can be also critical for EV. To address these aspects, a new variant of the active suspension has been developed for the target vehicle. It has electro-hydraulic layout and includes also air dampers, Fig. 5. The corresponding measures for energy efficiency optimization led to the following power consumption data in the case of the system operation: max. continuous electrical power is  $\pm 500$  W / vehicle or  $\pm 125$  W / actuator, with on-board power supply short-term peak power of max.  $\pm 3.5$  kW / vehicle or  $\pm 1.2$  kW / actuator.

### 5. INTEGRATED CONTROL

The powertrain and chassis components, described in the previous sections, are involved in various functions of the integrated control on the EV dynamics, which includes such functions as torque vectoring<sup>(4)</sup>, drivability and wheel slip control<sup>(5)</sup>, and ride control<sup>(6)</sup>. To achieve the optimal power management, the named high level controls get enhanced with torque blending functionality. This e.g. allows the usage of the IWMs while braking, which is beneficial in consequence of their high dynamics. Fig. 6 shows the interaction of the different blocks in a schematic manner, wherein the inputs on the left side represent components' CAN busses and the shown parameters are specified as follows. Parameters with a hat index get not directly measured, but estimated by the observer blocks.

First signals to mention are the driver inputs, where  $s_{Ped,br}$  and  $s_{Ped,acc}$  are the stroke of the brake or accelerator pedal, respectively, and  $\delta_{SW}$  is the steering wheel angle. Next parameters are  $m_v$  as the total vehicle mass,  $v_x$  as its longitudinal speed and  $\chi$  which describes the percentual road slope. The values of  $F_x, F_y, F_z$  and  $\lambda_x$  represent the tire forces in longitudinal, lateral and vertical direction and also the wheel slip ratio. The indices code the corresponding wheel, where  $i$  stands for the axle and  $j$  for the side. By inserting the previous mentioned signals in the "Reference Generator" block, the total torque demand  $T_{dem}$  and the front-to-total distribution  $f_i^{ECE}$  are calculated. The parameter  $\dot{\psi}_{dem}$  is the yaw rate related to applied the steering angle. These signals get

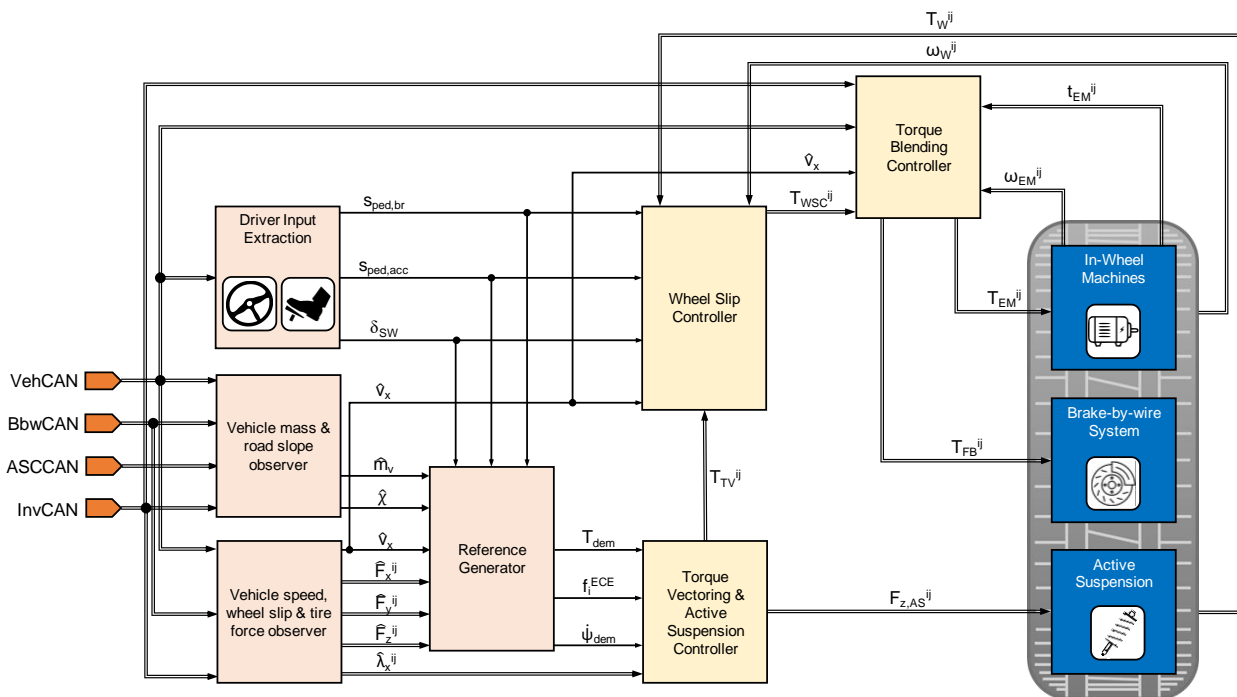


Fig. 6 Block scheme of integrated chassis controller

forwarded to “Torque Vectoring and Active Suspension Control” block, where the demanded torque  $T_{TV}$  and the vertical counterforce for the electro-hydraulic dampers  $F_{z,AS}$  get generated. Latter is directly applied to the active suspension system, while the other parameter has to be corrected by the “Wheel Slip Control” block, where the wheel slip is adapted to its optimum for maximum traction. Therefore, the demanded torque  $T_{TV}$  and additionally the feedback torque from the wheels ( $T_w$ ) and also resulting wheel speeds ( $\omega_w$ ) are taken into account, respectively. The slip limited torque  $T_{WSC}$  is now forwarded to the “Torque Blending Control” block, wherein the requested torque is divided into regenerative and friction braking part and applied to the IWMs and friction brakes by the signals  $T_{EM}$  and  $T_{FB}$ . Moreover, the motor state, given by its rotational speed ( $\omega_{EM}$ ) and the wiring temperature ( $t_{EM}$ ), is considered by torque blending controller.

Another important advancement of the proposed controller consists in the embedding connectivity functions to allow the maximum possible energy saving over a broader range of driving situations or use cases. This feature is based on the Travel Light Assistance and an energy-efficient Cooperative Adaptive Cruise Control<sup>(7)</sup> using V2V-communication. The full version of the paper will introduce the main elements and analytical formulation of the integrated controller.

### 6. TEST RESULTS

The final section of the paper will present selected validation and test results illustrating both the performance of powertrain / chassis components and the vehicle operation in particular use cases. Since Fig. 6 depicts the torque vectoring controller as the first relevant institution after torque demand generation, it will be explained first.

#### Torque Vectoring Control & Active Suspension Control

Torque vectoring (TV) consists on the control of the wheel torque levels to influence the yaw rate, and in second instance the energy consumption. This enhances vehicle lateral stability and agility during cornering. As mentioned in section 4, the IWMs increase the unsprung mass, which can lead to decreased road holding and ride comfort on irregular road profiles. Therefore, the EVC1000 demonstrator vehicle is additionally equipped with an active suspension system, see Fig. 5. Differently from passive or even semi-active devices, active suspension systems are able to actively suppress the dynamic vertical forces induced by road irregularities, which is leading to remarkable ride comfort improvements. Moreover, suspension control can be used to

reduce the roll motion in cornering conditions, which is beneficial to lateral stability as well.

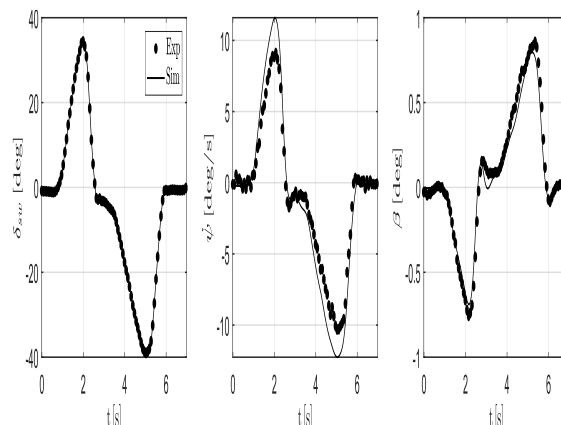


Fig. 7 Polynomial fitting of the measured IWM power losses.

Fig. 8 reports the battery power increase  $P_{batt,inc}$  relative to the most effective combination of 4WD vehicle with combined torque vectoring and active suspensions control for longitudinal accelerations of  $a_x = 0 \text{ m/s}^2$  (upper) and  $a_x = 1.5 \text{ m/s}^2$  (lower).

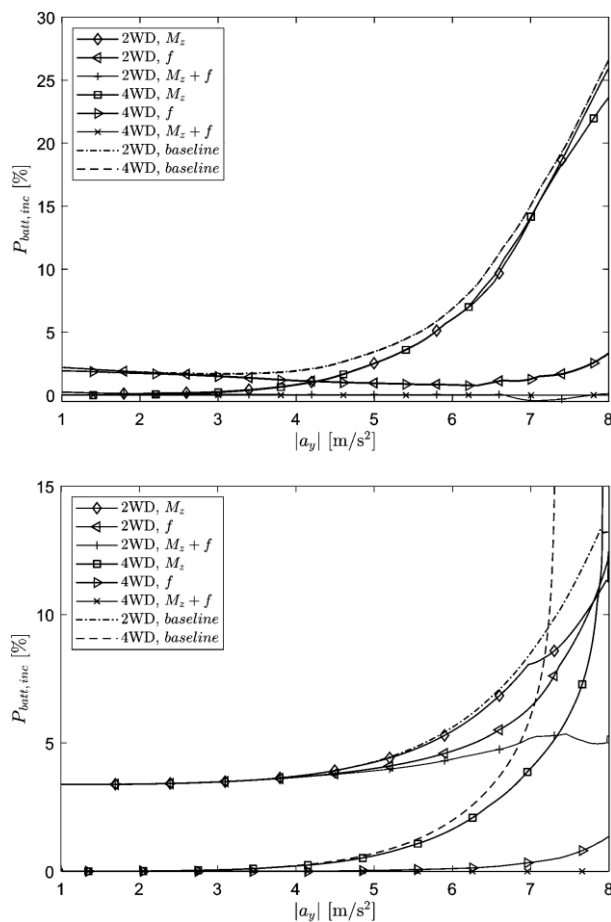


Fig. 8 Power increase in relation to lateral acceleration associated to different chassis actuation sets.

The discussed experiments achieved, that torque vectoring is beneficial up to medium lateral accelerations, where the active suspensions do not give any appreciable effects owing to the negligible lateral load transfer, whereas the active roll-moment distribution becomes significantly more efficient at higher lateral accelerations.

The front-to-total anti-roll moment distribution can be tuned to enhance the vehicle cornering response through active suspension control, i.e., an increase of the front anti-roll moment and a reduction of the rear anti-roll moment increase understeer, while a decrease of the front anti-roll moment and an increase of the rear anti-roll moment reduce understeer. The EVC1000 active suspension system continuously varies the anti-roll moment distribution to achieve desirable yaw rate response.

In the EVC1000 implementation, both the torque vectoring and active suspension controller are based on an implicit non-linear model predictive control (NMPC) approach, and tuned towards energy efficiency. Therefore, the cost function of the controller considers the sum of all relevant mechanical and electrical power losses. In particular, Fig. 7 shows the IWM power loss map (grey points) and its polynomial approximation (black grid) used for NMPC implementation.

The activity included the simulation-based analysis of the power consumption benefits in cornering conditions, associated with different vehicle configurations. For example, Fig. 8 reports the battery power increase,  $P_{batt,m}$ , relative to the most effective combination of 4WD vehicle with combined torque vectoring (indicated by  $M_z$ ) and active suspension (indicated by  $f$ ) control for longitudinal accelerations  $a_x = 0 \text{ m/s}^2$  (upper plot) and  $a_x = 1.5 \text{ m/s}^2$  (lower plot). Torque vectoring is especially beneficial up to medium lateral accelerations, where the active suspensions do not give any noticeable effects owing to the negligible lateral load transfer. On the contrary, the active roll-moment distribution makes the vehicle significantly more efficient at higher lateral accelerations. The analysis also included the potential power consumption benefits associated with rear wheel steering control.

The previous controllers were additionally enhanced by a vibration attenuation functionality, which corresponds to the reduction of the influence of road irregularities on ride comfort. In fact, IWMs and their excellent torque dynamics characteristics are suitable for damping the longitudinal acceleration oscillations associated with road irregularities. At the same time, the active suspension system can be used for the compensation of the vertical body oscillations. Therefore, EVC1000 developed NMPC

formulations for longitudinal and vertical motion control, based on the preview of the road profile ahead.

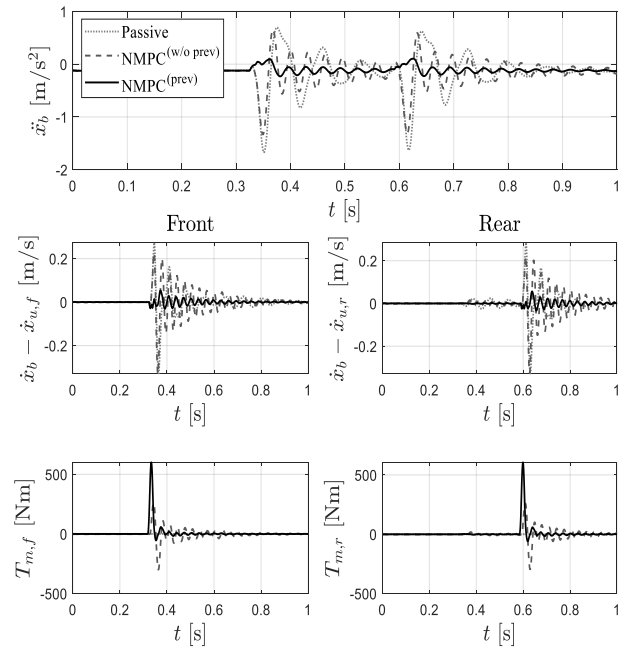


Fig. 9 Example of results with and without the longitudinal vibration attenuation controller, implemented with ('prev') or without ('w/o prev') road profile preview. Top: longitudinal acceleration profiles; centre: relative longitudinal speed between sprung and unsprung masses; bottom: IWM torque profiles

Fig. 9 reports preliminary results of the longitudinal vibration attenuation performance for a road input step, with respect to the uncontrolled system. The oscillations of the longitudinal acceleration are remarkably lower than without control. A sensitivity analysis was used to determine the most appropriate values of prediction horizon and preview time.

### Torque Blending

Besides its capability to compensate longitudinal oscillations, electric propulsion also offers many other advantages for vehicle dynamics and control engineering. One remarkable point is the energy recovery in generator mode, which allows recharging of the traction battery. This regenerative braking is beneficial for mileage and can be used for most comfort brake manoeuvres (up to nearly 0.3g of deceleration) to reduce particle emissions of the brakes and tires and also to extend the brakes life-time. For higher deceleration requests or in case of any other constraints (battery state, motor speed and temperature, etc.), the friction brakes are used to cover the lack of torque demand. The intelligent mixture is known as "torque blending". In the present case, a parameter,

namely *blending factor*  $\alpha$  was introduced to control the torque distribution. Fig. 10 depicts the variation of this parameter as reaction to predefined constraints.

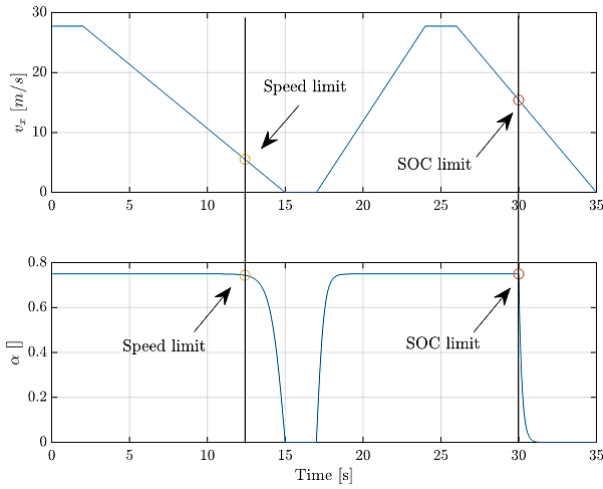


Fig. 10 Consideration of blending constraints

### Wheel Slip Control

As the blending controller aims to provide the maximum available torque to the wheels, which leads to excessive skid or spin of the wheel, a wheel slip controller is needed in addition.

The realized controller is based on continuous control approaches, namely Proportional-Integral with anti-windup part (PI) and integral sliding mode (ISM), which have remarkable advantages in regard of the ABS key performance indicators (KPIs) against the classical rule-based one<sup>(8)</sup>. In Fig. 11 and Fig. 12 the results of a comparative case study under real-time conditions are shown for straight-line-braking manoeuvres under different circumstances. Depicted are the KPIs for evaluation of vehicle safety, vehicle stability and ride comfort. The first six scenarios were performed under high- $\mu$  and low- $\mu$  conditions at different pedal appliance speeds, test cases 7 and 8 on  $\mu$ -split road and test case 9 on patches with different friction coefficients<sup>(9)</sup>.

Especially the results of the test cases 7 to 9 are quite interesting, because braking distance becomes less important for evaluation than vehicle stability, which is characterized by the root-mean square error (RMSE) of the yaw rate. Background is, that a vehicle tends to turn around its  $z$ -axis because of emerging yaw moment by different longitudinal forces on left and right wheels while braking on inhomogeneous road surfaces as specified in those scenarios.

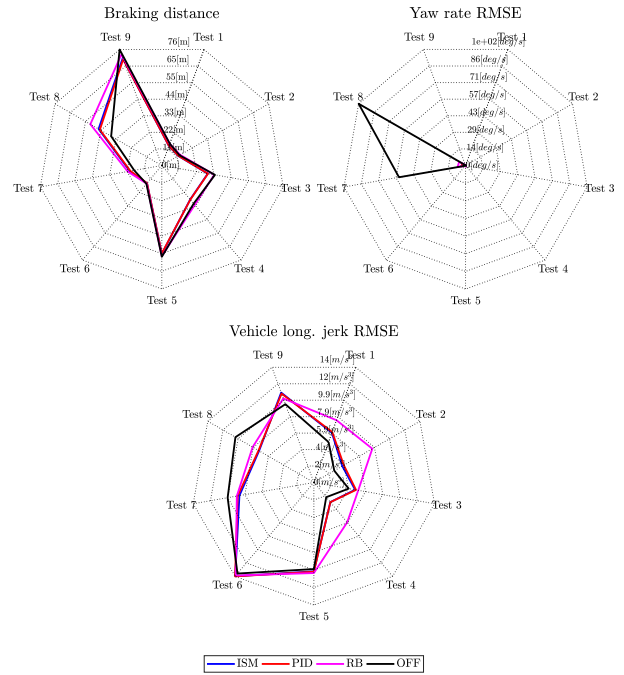


Fig. 11. Radar plots with deactivated torque blending

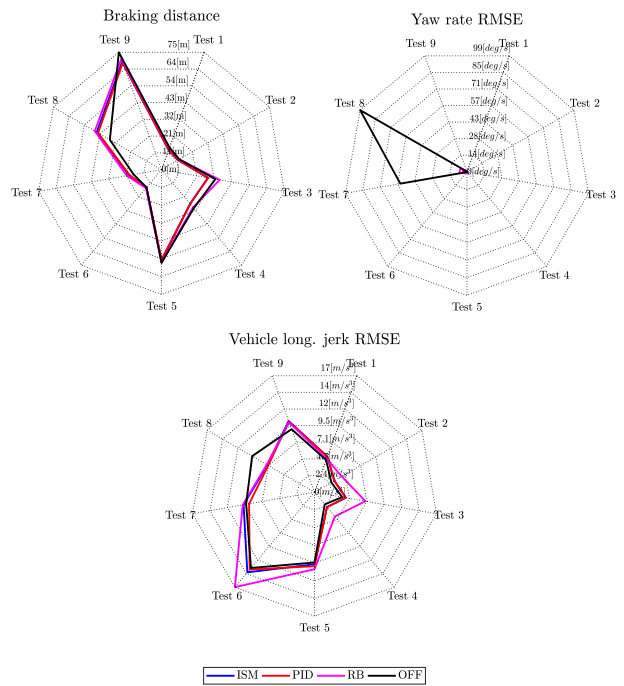


Fig. 12. Radar plots with activated torque blending

Summarized, the following results have been achieved:

- On homogeneous undergrounds, the PI and ISM control decrease braking distance;
- Continuous approaches improve lateral stability on  $\mu$ -split road compared to classical rule-based control;
- Using electric motors for wheel slip control is advantageous for ride comfort.

### Cooperative Adaptive Cruise Control (CACC)

This controller combines the functionality of classical Adaptive Cruise Control and Vehicle-to-X communication technology. The new cooperative ACC (CACC) adapts vehicle dynamics based on information of preceding traffic and also of traffic light signal periods. This approach shall increase energy efficiency, vehicle safety and ride comfort without too extensive travelling time.

The first set of results in Fig. 13 shows a highway scenario, where the target follows another preceding vehicle. The graph shows less excessive acceleration and deceleration manoeuvres which tends to lower longitudinal jerk which is a direct comfort index. Regarding the energy consumption, the CACC shows less energy demand for performing the manoeuvre. In this test case, the CACC achieves energy savings of 16.7 % with a travel time loss of 0.1 % and a jerk RMS reduction of 46 %.

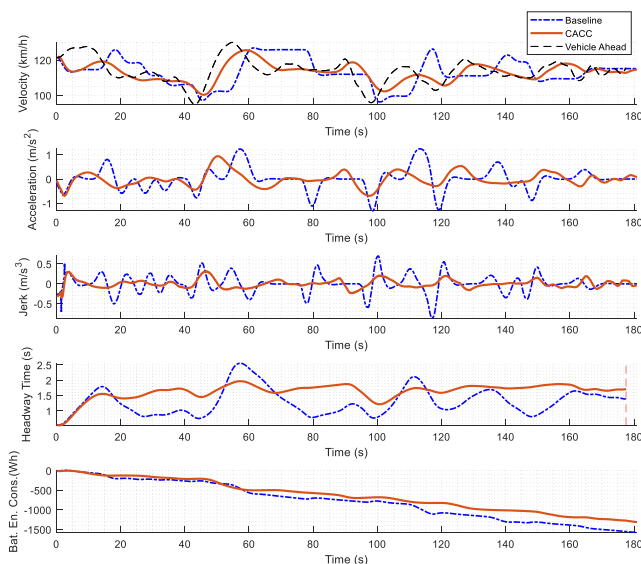


Fig. 13 Highspeed Scenario with preceding traffic

In the second manoeuvre, the ego vehicle follows the preceding target in an urban environment including also traffic lights. The results, Fig. 14, show, that the CACC works more efficient and is also able to avoid stopping at several traffic lights due to its informations provided over V2X communication. Most of the reductions in relative savings in this test case arise already at the first traffic light, where the CACC is forced to decelerate to approximately 25 km/h due to the preceding vehicle which is at standstill. The CACC achieves significantly improved energy savings and driver comfort, with a basically unchanged travel time compared to a simulated human driver.

Please note, that the degree of regenerative braking reduces the energy consumption and influences the CACC's relative energy

savings. For all the test cases, the blending factor was set to  $\alpha = 0.33$ , means that 33% of the requested brake torque was covered by the electric machines. Higher factors can lead to 30 per cent less improvement.

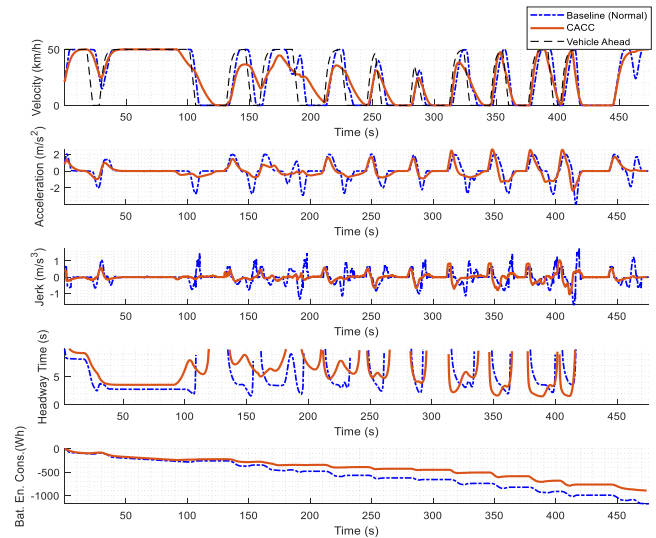


Fig. 14 Urban scenario with traffic lights and preceding traffic

### ACKNOWLEDGMENT

This project has received funding from the European Union's Horizon 2020 research and innovation programme under grant agreement No 824250.

### REFERENCES

- (1) L. Cozzi and A. Petropoulos, "Growing preference for SUVs challenges emissions reductions in passenger car market," *International Energy Agency (IEA) Report*, Paris, 2019.
- (2) <http://www.evc1000.eu/en> (accessed September 19, 2020)
- (3) B. Modic, U. Skrt, T. Motaln, G. Lampič, and G. Gotovac, "In-wheel Powertrain Functions for the Autonomous and Connected Future - Advanced Powertrain Functionalities Enabling New Possibilities for the Future of Mobility," *Proceedings of EVS 31 & EVTec 2018*, pp. 1-7, Kobe, Japan, Sep 30 – Oct 03 2018.
- (4) M. Metzler, D. Tavernini, A. Sorniotti, and P. Gruber, "Explicit non-linear model predictive control for vehicle stability control," *Proceedings of the 9th International Munich Chassis Symposium*, 2018.
- (5) M. Heydrich, V. Ricciardi, V. Ivanov, and K. Augsborg, "Robust design of combined control strategy for electric vehicle with in-wheel propulsion," *Proceedings of IEEE VPPC 2020*, Gijón, Spain, Oct 26 – 29 2020.

- (6) J. Theunissen, A. Sorniotti, P. Gruber, S. Fallah, M. Ricco, M. Kvasnica, and M. Dhaens, "Regionless Explicit Model Predictive Control of Active Suspension Systems with Preview," *IEEE Transactions on Industrial Electronics*, vol. 67, no. 6, pp. 4877-4888, 2020.
- (7) N. Wikström, A. Ferreira Parrila, S. J. Jones, and A. Grauers, "Energy-Efficient Cooperative Adaptive Cruise Control with Receding Horizon of Traffic, Route Topology, and Traffic Light Information", *SAE International Journal of Connected and Automated Vehicles*, vol. 2, no. 2, pp. 87-98, 2019.
- (8) F. Pretagostini, L. Ferranti, G. Berardo, V. Ivanov, and B. Shyrokau, "Survey on Wheel Slip Control Design Strategies, Evaluation and Application to Antilock Braking Systems", *IEEE Access*, vol. 8, pp. 10951-10970, 2020.
- (9) M. Heydrich, V. Ricciardi, V. Ivanov, M. Mazzoni, A. Rossi, J. Buh, and K. Augsburg, "Integrated Braking Control for Electric Vehicles with In-Wheel Propulsion and Fully Decoupled Brake-by-Wire System", *Vehicles*, vol. 3, no. 2, pp. 145-161, 2021.